THE JOURNAL OF BIOLOGICAL CHEMISTRY VOL. 291, NO. 12, pp. 6507–6520, March 18, 2016

A Human Disease-causing Point Mutation in Mitochondrial Threonyl-tRNA Synthetase Induces Both Structural and Functional Defects*

Received for publication, October 27, 2015, and in revised form, January 5, 2016 Published, JBC Papers in Press, January 25, 2016, DOI 10.1074/jbc.M115.700849

Yong Wang[‡§1], **Xiao-Long Zhou**[‡1,2], **Zhi-Rong Ruan**[‡1], **Ru-Juan Liu**[‡], **Gilbert Eriani**[¶], **and En-Duo Wang**[‡§3]

From the [‡]*State Key Laboratory of Molecular Biology, Chinese Academy of Sciences Center for Excellence in Molecular Cell Science, Institute of Biochemistry and Cell Biology, Shanghai Institutes for Biological Sciences, University of Chinese Academy of Sciences, Shanghai 200031, China, the* [§]*School of Life Science and Technology, ShanghaiTech University, 319 Yue Yang Road, Shanghai 200031, China, and the* [¶]*Architecture et Réactivité de l'ARN, UPR9002 CNRS, Institut de Biologie Moléculaire et Cellulaire, Université de Strasbourg, 15 rue René Descartes, 67084 Strasbourg, France*

Mitochondria require all translational components, including aminoacyl-tRNA synthetases (aaRSs), to complete organelle protein synthesis. Some aaRS mutations cause mitochondrial disorders, including human mitochondrial threonyl-tRNA synthetase (hmtThrRS) (encoded by *TARS2*), the P282L mutation of which causes mitochondrial encephalomyopathies. However, its catalytic and structural consequences remain unclear. Herein, we cloned *TARS2* and purified the wild-type and P282L mutant hmtThrRS. hmtThrRS misactivates non-cognate Ser and uses post-transfer editing to clear erroneously synthesized products. *In vitro* and *in vivo* analyses revealed that the mutation induces a decrease in Thr activation, aminoacylation, and proofreading activities and a change in the protein structure and/or stability, which might cause reduced catalytic efficiency. We also identified a splicing variant of *TARS2* mRNA lacking exons 8 and 9, the protein product of which is targeted into mitochondria. In HEK293T cells, the variant does not dimerize and cannot complement the ThrRS knock-out strain in yeast, suggesting that the truncated protein is inactive and might have a non-canonical function, as observed for other aaRS fragments. The present study describes the aminoacylation and editing properties of hmtThrRS, clarifies the molecular consequences of the P282L mutation, and shows that the yeast ThrRS-deletion model is suitable to test pathology-associated point mutations or alternative splicing variants of mammalian aaRS mRNAs.

Aminoacyl-tRNA synthetases (aaRSs)[4] supply the ribosome with aminoacyl-tRNA substrates for protein synthesis (1, 2). This process starts with amino acid activation by condensation with ATP to form the aminoacyl adenylate aa-AMP and pyrophosphate. The activated amino acid then reacts with the 3′-end of the cognate tRNA to yield the aminoacyl-tRNA (aa-tRNA), which is transferred by EF-Tu to the protein biosynthesis machinery as a building block. Highly accurate protein synthesis is indispensable for cell growth. To maintain fidelity during protein synthesis, aaRS needs to select the correct amino acid and tRNA substrates from a large number of structurally similar molecules in the cells. The specificity of aaRS is greatly challenged by the presence of the 20 amino acids in which the physicochemical properties are sometimes very similar and by non-proteogenous amino acids and diverse metabolites produced by cell metabolism. aaRSs that do not show an overall selectivity above 1 in 3000 are predicted to require proofreading (editing) activity to maintain sufficient accuracy during aa-tRNA synthesis (3). In fact, editing activity has evolved in half of the currently identified aaRS to remove aberrantly produced aa-AMP (pretransfer editing) and/or aa-tRNA (post-transfer editing) (4). tRNA mischarging may be toxic and deleterious for cells. Even a slight decrease in aminoacylation accuracy could cause an intracellular accumulation of misfolded proteins and up-regulation of cytoplasmic protein chaperones in neurons, leading to severe mammalian neurodegeneration (5). Mistranslation arising from disruption of translational fidelity also has profound consequences in *Escherichia coli* (6, 7) and mammalian cells (8).

Mitochondria play a key role in cell growth, such as the regulation of nitrogen metabolism and programmed cell death (9). In addition, they provide most of the cellular energy by oxidative phosphorylation (OXPHOS) and act as cellular power plants. In particular, mitochondria possess their own genome. Human mitochondrial DNA (mtDNA) is a small circular molecule of 16,569 bp. It encodes 13 polypeptides that are essential subunits of respiratory complexes, 22 tRNA, and two rRNA (10, 11). Except for two $tRNA^{Leu}$ or $tRNA^{Ser}$ iso-acceptors, the other amino acids have only one corresponding tRNA (such as one mitochondrial $tRNA^{Thr}$(UGU)) for protein synthesis. MtDNA undergoes mutations at a higher rate than nuclear genomes because of the presence of reactive oxygen species, its freedom from histones, and lack of repair mechanisms (12, 13). Over the last decade, more than 200 point mutations and rear-

* This work was supported by Grant 2012CB911000 from the National Key Basic Research Foundation of China, Grants 31130064 and 91440204 from the Natural Science Foundation of China, and Grants 12JC1409700 and 15ZR1446500 from the Committee of Science and Technology in Shanghai. This work was also supported by the Youth Innovation Promotion Association (Chinese Academy of Sciences) (to X. L. Z.). The authors declare that they have no conflicts of interest with the contents of this article.

[1] These authors contributed equally to this work.
[2] To whom correspondence may be addressed. Tel.: 86-21-54921242; Fax: 86-21-54921011; E-mail: xlzhou@sibcb.ac.cn.
[3] To whom correspondence may be addressed. Tel.: 86-21-54921241; Fax: 86-21-54921011; E-mail: edwang@sibcb.ac.cn.

[4] The abbreviations used are: aaRS, aminoacyl-tRNA synthetase; ThrRS, threonyl-tRNA synthetase; hmtThrRS, human mitochondrial ThrRS; hctRNA, human cytoplasmic tRNA; *Sc*ThrRS, *Saccharomyces cerevisiae* ThrRS; *Ec*ThrRS, *Escherichia coli* ThrRS; qPCR, quantitative real-time PCR; MTS, mitochondrial targeting sequence; 5-FOA, 5-fluoroorotic acid.

rangements associated with a large number of a wide spectrum of clinical abnormalities have been reported (14). However, over half of these mutations occurred in tRNA genes (15). In addition, mitochondrial aaRSs encoded by the nuclear genome are key components of the mitochondrial protein synthesis system. They are synthesized in the cytoplasm, imported into and function in the mitochondria (16).

ThrRSs are present in all three domains of life and usually contain an N-terminal N1 domain, an N2 domain (for editing), an aminoacylation domain (for amino acid activation and tRNA charging), and an anticodon binding domain (for tRNA binding) (17). Based on an alignment of primary sequences, bacterial ThrRSs display an obvious difference to eukaryotic ThrRSs in the N-terminal N1 and N2 (editing) domains. Interestingly, despite the bacterial origin of mitochondria, human mitochondrial ThrRS (hmtThrRS) is more similar to eukaryotic cytoplasmic ThrRS. hmtThrRS is encoded by the *TARS2* gene. Bacterial and eukaryotic cytoplasmic ThrRS, shown to misactivate non-cognate Ser, mainly use an efficient post-transfer editing activity to clear mischarged Ser-tRNA^{Thr} in addition to tRNA-dependent pretransfer editing (18–20). In contrast, *Saccharomyces cerevisiae* mitochondrial ThrRS (*Sc*mtThrRS) naturally lacks an editing domain and only harbors tRNA-independent and tRNA isoacceptor-specific pretransfer editing (21, 22). As a result, *Sc*mtThrRS lacks post-transfer editing and is an error-prone synthetase, forming Ser-tRNA^{Thr}, at least *in vitro* (22). Several bacterial or cytoplasmic aaRSs are critically dependent upon their editing activity to achieve accurate aminoacylation. However, in several cases, the corresponding human mitochondrial enzymes carry non-functional editing sites or lack editing domains, raising the question of their aminoacylation fidelity. In fact, these enzymes achieve fidelity using a more specific amino acid binding pocket, reducing the need of editing activity. This enhanced specificity compensating for the presence of a defunct editing site has been identified in human mitochondrial LeuRS (23) and *S. cerevisiae* mitochondrial PheRS (24, 25).

Concerning hmtThrRS encoded by *TARS2*, no information is available on its aminoacylation and editing activities. According to the increasing number of mutations in aaRS genes causing mitochondrial dysfunctions, including hmtThrRS (26), there is an interest in analyzing the functional properties of these molecules and developing new tools to examine their *in vivo* properties. Recently, two mutations (c.845C>T, encoding hmtThrRS-P282L and a nucleotide change in position +3 of intron 6 (g.4255A>G; c.695 + 3A>G)) were identified in *TARS2* in two siblings presenting axial hypotonia and severe psychomotor delay associated with multiple mitochondrial respiratory chain defects (26). Both hmtThrRS protein and aminoacylated tRNA^{Thr} levels are decreased in the patients' cells. The g.4255A>G mutation has no influence in mRNA splicing (26); therefore, it was proposed that the c.845C>T mutation is responsible for patient phenotypes. However, how the mutation affects protein structure, stability, and catalytic activities remains largely unknown.

In this study, we cloned *TARS2*, encoding the hmtThrRS precursor, and purified soluble hmtThrRS. In yeast, we found that the only *S. cerevisiae* tRNA^{Thr} is not an efficient substrate for hmtThrRS. To be used as an *in vivo* functional assay in yeast, we found that an extra human tRNA had to be added. We also showed that hmtThrRS misactivates non-cognate Ser, and a robust pretransfer editing, in addition to post-transfer editing, prevents the formation of mischarged tRNA. In addition, we explored the effect of mutation of Pro^{282} in detail and found that the mutant hmtThrRS-P282L causes an obvious decrease in amino acid activation, tRNA^{Thr} aminoacylation, and editing. Furthermore, we revealed that the mutation alters the structure and/or stability of the protein. Finally, in several cell lines, we identified a splicing variant of *TARS2* encoding a truncated, catalytically inactive hmtThrRS. The variant is readily translated and imported into mitochondria, suggesting a noncanonical mitochondrial function. This phenomenon is reminiscent of other examples of synthetase fragments and supports the hypothesis that alternative splicing of mRNA transcripts of aaRS is a way to enlarge aaRS additional functions in higher eukaryotes (27, 28). Altogether, our results significantly improve our understanding of hmtThrRS and provide a basis for further investigations of *TARS2*-related human diseases.

Experimental Procedures

Materials—L-Thr, L-Ser, dithiothreitol, NTP, GMP, tetrasodium pyrophosphate, inorganic pyrophosphate, Tris-base, $MgCl_2$, NaCl, and activated charcoal were purchased from Sigma. [^{14}C]Thr was obtained from Biotrend Chemicals (Destin, FL), and [^{14}C]Ser and [α-^{32}P]ATP were obtained from PerkinElmer Life Sciences. The DNA fragment rapid purification kits and plasmid extraction kits were purchased from Yuanpinghao Biotech. KOD-plus mutagenesis kits were obtained from Toyobo. T4 DNA ligase and restriction endonucleases were obtained from Thermo Fisher Scientific. Phusion high-fidelity DNA polymerase was purchased from New England Biolabs. Ni^{2+}-NTA Superflow was purchased from Qiagen Inc. Polyethyleneimine cellulose plates were purchased from Merck. Pyrophosphatase (PPiase) was obtained from Roche Applied Science. The dNTP mixture was obtained from Takara. Oligonucleotide primers were synthesized by Invitrogen. *E. coli* BL21(DE3) cells were purchased from Stratagene. The yeast transformation kit was purchased from Clontech. Mouse anti-FLAG (M20008, anti-His_6 tag (M20001), anti-GAPDH (M20028), and anti-c-Myc (M20002) antibodies were purchased from Abmart.

Gene Cloning, Mutagenesis, Expression, and Protein Purification—The *TARS2* coding sequence was amplified from cDNA obtained by RT-PCR from total RNA obtained from HEK293T cells and cloned into pET28a(+) with an N-terminal His_6 tag and named pET28a(+)-*TARS2*. pET28a(+)-*TARS2* was used as the template to construct N-terminal truncation mutants. Gene mutagenesis was performed according to the protocol provided with the KOD-plus mutagenesis kit. *E. coli* BL21(DE3) was transformed with various constructs. Protein purification was performed according to a previously described method (29).

tRNA Gene Cloning and Transcription—The DNA sequences of the T7 promoter and the hmttRNA^{Thr}(UGU) gene were obtained by ligating two chemically synthesized DNA fragments for each strand, which were then ligated into the

pTrc99b plasmid (precleaved with EcoRI/PstI) to construct pTrc99b-T7-hmttRNA^{Thr}(UGU). Then, the template was amplified for transcription *in vitro* using Phusion polymerase and the forward primer (5′ CACAGGAAACAGACCATGGGAATTC 3′) and reverse primer (5′ TGGTGTCCTTGGAAAAAGGTTTTCATCTC 3′). hmttRNA^{Thr} transcripts were obtained using the T7 RNA polymerase run-off procedure as described previously (7).

Yeast Complementation Assay, Preparation of Yeast Cell Lysates, and Western Blotting—For complementation assays, all genes of interest were cloned into the yeast expression vector, p425TEF and fused with a DNA fragment encoding a C-terminal His_6 tag to facilitate protein level determination using an anti-His_6 antibody. The hmtThrRS construct or the hmtThrRS plus hctRNA^{Thr}(AGU) constructs were transformed separately into the *Sc*Δ*thrS* strain (BY4743, *thrS*$^-$, pRS426-*Sc*ThrRS). Transformants were selected on SD/Ura$^-$/Leu$^-$ plates or SD/Ura$^-$/Leu$^-$/His$^-$ plates (for co-expression of hctRNA^{Thr}(AGU)), and a single clone was cultured in liquid SD/Leu$^-$ or SD/Leu$^-$/His$^-$ medium. The culture was then diluted to a concentration of 1 OD_{600} (5×10^7 cells/ml); a 10-fold dilution series of the yeast cells was plated onto the SD/Leu$^-$/5-FOA or SD/Leu$^-$/His$^-$/5-FOA medium to induce the loss of the rescuing plasmid (pRS426-*Scthr*S) and was grown for 3 days on 30 °C. The same procedure was used to check whether hmtThrRS variants could support the growth of the *Sc*Δ*thrS* strain.

Yeast transformants were grown in liquid SD/Leu$^-$/Ura$^-$ or SD/Leu$^-$/Ura$^-$/His$^-$. Yeast cells were lysed following a previously described method (30). Recombinant proteins in the cell lysates were detected by Western blotting with anti-His_6 antibodies.

ATP-PP$_i$ Exchange Assay—The ATP-PP$_i$ exchange measurement was carried out at 37 °C in a reaction mixture containing 60 mM Tris-HCl (pH 7.5), 10 mM $MgCl_2$, 5 mM DTT, 0.1 mg/ml BSA, 2.5 mM ATP, 2 mM tetrasodium [^{32}P]pyrophosphate, 0.5–20 mM Thr or 50–800 mM non-cognate Ser, and 200 nM hmtThrRS or its variants. Samples of the reaction mixture were removed at specific time points and added into 200 μl of quenching solution containing 2% activated charcoal, 3.5% $HClO_4$, and 50 mM tetrasodium pyrophosphate. The solution was filtered through a Whatman GF/C filter followed by washing with 20 ml of Milli-Q water and 10 ml of 100% ethanol. The filters were dried, and [^{32}P]ATP was counted in a scintillation counter (Beckman Coulter).

Aminoacylation and Misaminoacylation—Aminoacylation kinetics were performed at 37 °C in a reaction mixture containing 60 mM Tris-HCl (pH 7.5), 10 mM $MgCl_2$, 5 mM DTT, 0.1 mg/ml BSA, 2.5 mM ATP, 100 μM [^{14}C]Thr, 0.5–10 μM hmttRNA^{Thr}, and 200 nM hmtThrRS or its variants. Misaminoacylation of hmttRNA^{Thr} with [^{14}C]Ser was carried out at 37 °C in a reaction mixture containing 60 mM Tris-HCl (pH 7.5), 10 mM $MgCl_2$, 5 mM DTT, 2.5 mM ATP, 0.1 mg/ml BSA, 160 μM [^{14}C]Ser, 5 μM hmttRNA^{Thr}, and 2 μM hmtThrRS or hmtThrRS-H133A/H137A.

^{32}P Labeling of hmttRNA^{Thr} and Preparation of Ser-[^{32}P]hmttRNA^{Thr}—We performed the ^{32}P labeling of hmttRNA^{Thr} at 37 °C in a mixture containing 60 mM Tris-HCl (pH 8.0), 10 mM $MgCl_2$, 10 μM hmttRNA^{Thr}, 0.5 mM DTT, 5 μM ATP, 50 μM tetrasodium pyrophosphate, 0.66 μM [α-^{32}P]ATP, and 10 μM CCA-adding enzyme (CCase) for 5 min. Then, 0.1 unit of PPiase was added to the mixture for 5 min. The solution was extracted twice using phenol/chloroform and then precipitated in 3 volumes of ethanol.

[^{32}P]hmttRNA^{Thr} was incubated with Ser at 37 °C in a reaction mixture containing 60 mM Tris-HCl (pH 7.5), 10 mM $MgCl_2$, 2 mM DTT, 4 mM ATP, 5 μM unlabeled hmttRNA^{Thr}, 1.5 μM [^{32}P]hmttRNA^{Thr}, 500 mM Ser, and 10 μM hmtThrRS-H133A/H137A for 1 h. The solution was then extracted twice using acid phenol (pH4.5)/chloroform and precipitated in 3 volumes of 100% ethanol at −20 °C overnight. The precipitated sample was centrifuged (12,000 × *g*) at 4 °C for 30 min, dried at room temperature for 30 min, and dissolved in 5 mM $MgCl_2$. The ratio of Ser-[^{32}P]hmttRNA^{Thr} was determined by liquid scintillation counting of the sample washed with and without 5% trichloroacetic acid.

Post-transfer Editing—Post-transfer editing of preformed Ser-[^{32}P]hmttRNA^{Thr} was performed in a reaction mixture containing 60 mM Tris-HCl (pH 7.5), 10 mM $MgCl_2$, 1 μM Ser-[^{32}P]hmttRNA^{Thr}, and 200 nM hmtThrRS or its variants at 37 °C. Samples at specific time points were taken for ethanol precipitation with NaAc (pH 5.2) at −20 °C overnight. The precipitated samples were centrifuged (12 000 × *g*) at 4 °C for 30 min, dried at room temperature for 30 min, and digested with 6 μl of nuclease S1 (25 units) for 2 h at 37 °C. After nuclease S1 digestion, samples (2 μl) of the digestion mixture were loaded and separated by TLC in 0.1 M NH_4Ac and 5% acetic acid. The plates were visualized by phosphorimaging, and the data were analyzed using MultiGauge version 3.0 software (Fujifilm).

AMP Formation Assay—The AMP formation assay (using TLC) was carried out at 37 °C in a reaction mixture containing 60 mM Tris-HCl (pH 7.5), 10 mM $MgCl_2$, 5 mM DTT, 0.1 mg/ml BSA, 10 units/ml PPiase, 40 mM Ser (or 4 mM Thr), 3 mM [α-^{32}P]ATP, and 2 μM hmtThrRS or its variants in the presence and absence of hmttRNA^{Thr}. Samples (1.5 μl) at specific time points were quenched in 6 μl of 200 mM NaAc (pH 5.2). The quenched aliquots (1.5 μl of each sample) were spotted on polyethyleneimine cellulose plates prewashed with water. The separation of Ser-[α-^{32}P]AMP, [α-^{32}P]AMP, and [α-^{32}P]ATP was performed in 0.1 M NH_4Ac and 5% acetic acid. The plates were visualized by phosphorimaging, and the data were analyzed using MultiGauge version 3.0 software (Fujifilm). Quantification of [α-^{32}P]AMP was achieved by densitometry in comparison with [α-^{32}P]ATP samples of known concentrations.

Quantitative Real-time PCR (qPCR) of hmtThrRS-SV from cDNA Libraries of Different Cell Lines—hmtThrRS-SV was identified as a novel splicing variant of *TARS2* (see "Results"). Human total RNA from five cell lines was extracted using a TRIzol Plus RNA purification kit (Life Technologies) and then was used to synthesize cDNA libraries using the SuperScript III First Strand synthesis kit (Life Technologies). Primer pair 1, targeting exons 8 and 9, was used to detect the native transcripts: primer 1-F, CACAACAGAATTGCTGAGGG; primer 1-R, AGGGCTCAGTTCATGGAAGA. Primer pair 2, recognizing the exon 7/exon 10 boundary, was used to detect the hmtThrRS-SV transcripts: primer 2-F, GACAGGTCCAACAGCAACAG; primer 2-R, CATACTCAGCCGATAGCAGC.

qPCR was carried out using SYBR GreenER qPCR SuperMix kits (Life Technology) on an ABI 7500 instrument, set as follows: 1 min at 95 °C followed by 40 cycles of 95 °C for 15 s, 60 °C for 30 s, and then 72 °C for 45 s. A default melt curve program was run at the end of the qPCR cycles to verify the specificity of the PCR reaction. A single amplicon of the correct size of target DNA fragment was detected by agarose gel electrophoresis. The amplification efficiency was nearly 95%, which was determined from a calibration curve based on the Ct values and different concentrations of cDNA template. qPCR values obtained for each cell line were normalized to GAPDH mRNA levels. The relative amount of hmtThrRS-SV was calculated using the ΔΔCt method from the qPCR values of hmtThrRS and hmtThrRS-SV (31).

Cell Transfection and Fluorescence Microscopy—HEK293T cells were transfected with the FLAG-tagged constructs of pCMV-3Tag-3A-*TARS2* or pCMV-3Tag-3A-hmtThrRS-SV precursor according to a previously described method (32). After transfection for 24 h, cells were stained with 100 nM MitoTracker (Life Technologies, M-7512) for 20 min and then fixed in PBS containing 4% paraformaldehyde for 30 min. Fixed cells were blocked in PBS plus 0.1% Triton X-100 buffer containing 5% BSA and incubated with mouse anti-FLAG antibodies overnight at 4 °C. The cells were then immunostained with Alexa Fluor 647-conjugated donkey anti-mouse IgG (Jackson ImmunoResearch, 715-605--150) and the nuclear counterstain DAPI. Fluorescent images were taken and analyzed using an FV1000 confocal microscope (Olympus).

Co-immunoprecipitation and Western Blotting Assay—The coding sequences of *TARS2* and hmtThrRS-SV precursor were cloned into eukaryotic expression vectors pCMV-3Tag-3A (with a C-terminal 3× FLAG tag) and pCMV-3Tag-4A (with a C-terminal 3× c-Myc tag). Plasmid pCMV-3Tag-4A-hmtThrRS precursor, together with either pCMV-3Tag-3A-hmtThrRS precursor or pCMV-3Tag-3A, was co-transfected into HEK293T cells using Lipofectamine 2000 to express the genes of FLAG- or c-Myc-hmtThrRS as described previously (32). The same method was used to express the hmtThrRS-SV precursor coding sequence. After transfection for 36 h, cells were lysed and incubated with anti-FLAG antibodies to immunoprecipitate hmtThrRS, as described previously (32). Cell lysates and immune complexes were separated and immunoblotted with either anti-FLAG or anti-c-Myc antibody.

Filter Binding Assays—The complex formation of hmtThrRS and [^{32}P]hmttRNA^{Thr} or hmtThrRS-P282L and [^{32}P]hmttRNA^{Thr} was monitored using the classical filter binding method reported by Berg and co-workers (33, 34). A Millipore nitrocellulose membrane (0.22 μm) was equilibrated in washing buffer (50 mM potassium phosphate (pH 5.5), 50 mM $MgCl_2$) for at least 10 min before use. Radiolabeled [^{32}P]hmttRNA^{Thr} (20 nM, 25,000 cpm) was incubated in 50 μl of binding buffer (50 mM HEPES-KOH (pH 6.8), 30 mM KCl, 12 mM $MgCl_2$) in the presence of various concentrations of hmtThrRS or hmtThrRS-P282L for 30 min at 4 °C. Upon RNA-protein association, samples were filtered through the pre-equilibrated nitrocellulose membranes. The filters were then washed twice with 0.3 ml of the washing buffer and air-dried before radioactive quantification. All of the data were analyzed using GraphPad Prism software.

Circular Dichroism (CD) Analysis of hmtThrRS and hmtThrRS-P282L—CD spectroscopy experiments were performed on a Jasco J-715 spectropolarimeter between wavelengths 190 and 250 nm at room temperature. Samples (0.2 mg/ml) were diluted and incubated in the assay buffer (5 mM Tris-HCl (pH 8.0), 5 mM NaCl). A 0.1-cm path length was used, and spectra were accumulated over five scans. Background signals from the cuvette and the buffer were subtracted from each spectrum. The data were analyzed using OriginLab software.

Measurement of the Thermal Stability of hmtThrRS and hmtThrRS-P282L—hmtThrRS and hmtThrRS-P282L were heated at 50 °C for increasing incubation times (1, 2, 3, 4, 5, and 10 min) and kept on ice. The aminoacylation activity of the two proteins was then measured at 37 °C in a reaction mixture containing 60 mM Tris-HCl (pH 7.5), 10 mM $MgCl_2$, 5 mM DTT, 0.1 mg/ml BSA, 2.5 mM ATP, 100 μM [^{14}C]Thr, 5 μM hmttRNA^{Thr}, and 200 nM enzyme. The activity of the enzymes before heating was designated as 100%. All experiments were independently repeated three times.

Results

Cloning and Expression of TARS2—The hmtThrRS precursor, comprising 718 amino acid residues, is encoded by the nuclear gene *TARS2*, which is located at chromosome 1q21.3. *TARS2* is transcribed in the nucleus and translated in the cytoplasm, and then the hmtThrRS precursor is transported into mitochondria via its mitochondrial targeting sequence (MTS). As revealed by primary sequence alignment, the hmtThrRS precursor resembles eukaryotic ThrRS more than its bacterial counterparts, illustrated by the conservation of the N-terminal extension and N1 and N2 editing domains. Aminoacylation and the anticodon binding domains are conserved among eukaryotic and bacterial ThrRSs.

Despite its being identified almost 10 years ago (35), no study has reported the cloning and expression of *TARS2*. To predict the N-terminal sequence of the mature protein, we used the algorithm MITOPROT (47), which calculates the N-terminal protein region that supports an MTS and the cleavage site. MitoProt predicted an MTS from Met^1 to Leu^{38}. Therefore, we cloned the DNA sequence encoding Phe^{39}–Phe^{718} into pET28a(+). However, hmtThrRS-Δ_N38 exclusively formed inclusion bodies under various expression conditions, and changes in the expression vectors or strains did not improve the solubility of the protein. Assuming that the mature form of hmtThrRS might not start as predicted at residue 39, we constructed three sequential deletions targeting the N terminus to obtain hmtThrRS-Δ_N19, hmtThrRS-Δ_N25, and hmtThrRS-Δ_N58. The results showed that only hmtThrRS-Δ_N19 was successfully expressed in a soluble form and at a significant level. After purification, hmtThrRS-Δ_N19 reached over 95% purity (Fig. 1*A*) and displayed obvious activity in catalyzing ThrtRNA^{Thr} formation (Fig. 1*B*) (aminoacylation kinetics are presented in subsequent sections below). Its charging activity indicated that hmtThrRS-Δ_N19 should be a homodimer, like other ThrRS (36). This result suggested that the cleavage of the MTS from the hmtThrRS precursor takes place at or near this posi-

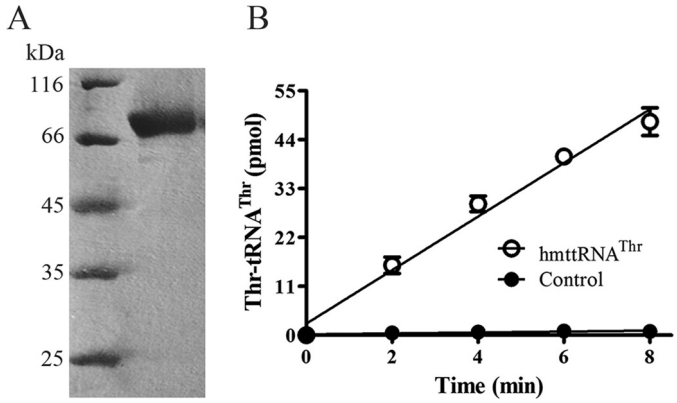

FIGURE 1. **Purification of an active hmtThrRS.** *A*, SDS-PAGE analysis of purified hmtThrRS. *B*, time course curve of aminoacylation of hmttRNA^{Thr} by hmtThrRS. The control was performed without enzyme addition. *Error bars*, S.D.

tion. Hereafter, hmtThrRS-Δ_N19 was used for enzymatic studies and was considered the "mature" form of hmtThrRS.

hmtThrRS Is Unable to Charge SctRNA^{Thr}(AGU) in Vitro and in Vivo—Nucleotides G^{35} and U^{36} in the anticodon loop and the discriminator base A^{73} are the typical recognition elements in the tRNA^{Thr} of bacterial, yeast cytosolic, and mitochondrial ThrRS (21, 37). One exception is the yeast mitochondrial tRNA^{Thr}1, which has an 8-nt anticodon loop harboring three extra identity elements: U^{33a}, G^{36}, and U^{38} (22). Human mitochondrial tRNA^{Thr} (hmttRNA^{Thr}(UGU)) is a normal-sized tRNA with an A^{73} discriminator base and a ^{34}UGU^{36} anticodon loop (Fig. 2*A*). Assuming that hmtThrRS exhibits the conserved set of identity elements of other ThrRS systems, we constructed three mutants targeting A^{73}, G^{35}, and U^{36} to validate their contribution during the process of tRNA recognition (Fig. 2*A*). The data showed that the G35C and U36C mutants could not be aminoacylated at all by hmtThrRS, whereas aminoacylation of A73C was partially decreased compared with wild-type hmttRNA^{Thr} (Fig. 2*B*). These data showed that nucleotides G^{35} and U^{36} are also critical recognition elements for the mitochondrial ThrRS and that A^{73} also plays a role. The three nucleotides A^{73}, G^{35}, and U^{36} are conserved in *S. cerevisiae Sc*tRNA^{Thr}(AGU), *Sc*tRNA^{Thr}(CGU), and *Sc*tRNA^{Thr}(UGU); therefore, we checked whether these nucleotides could manage aminoacylation of these tRNA^{Thr} by hmtThrRS. Surprisingly, despite the presence of these three nucleotides, the aminoacylation ability of *Sc*tRNA^{Thr}(CGU) and *Sc*tRNA^{Thr}(UGU) was strongly decreased, and *Sc*tRNA^{Thr}(AGU) was totally inactive (Fig. 2*C*). To rule out the possibility that the anticodon AGU could be responsible for this effect, we tested human cytosolic tRNA^{Thr}(AGU) (hctRNA^{Thr}(AGU)) harboring an identical AGU anticodon (Fig. 2*D*). Interestingly, hctRNA^{Thr}(AGU) was charged as efficiently as *Sc*tRNA^{Thr}(CGU) and *Sc*tRNA^{Thr}(UGU) (Fig. 2*C*), which suggested that some anti-determinant(s) exists in *Sc*tRNA^{Thr}(AGU) against hmtThrRS or that some unidentified determinant of aminoacylation is missing in this tRNA.

In a previous study, we reported that the gene *TARS2*-Δ_N38 was unable to rescue a yeast strain with a *thrS* knock-out (*Sc*Δ*thrS*) (20). As *TARS2*-Δ_N38 was not properly folded and remained insoluble in yeast (data not shown), we tested whether the newly identified deletion *TARS2*-Δ_N19 was able to rescue the strain *Sc*Δ*thrS*. However, under the same conditions, *TARS2*-Δ_N19 also failed to rescue the knock-out strain (Fig. 2*E*). Considering the inability of hmtThrRS to aminoacylate *Sc*tRNA^{Thr}(AGU) *in vitro* (see above), we hypothesized that ACU codons cannot be properly decoded *in vivo*, leading to the lethality of strain *Sc*Δ*thrS*. Indeed, *S. cerevisiae* harbors 17 genes for tRNA^{Thr}, among which 11 are for tRNA^{Thr}(AGU), demonstrating its abundance and crucial importance for protein translation in yeast. To this end, we simultaneously expressed *TARS2*-Δ_N19 or *TARS2*-Δ_N38 and the human hctRNA^{Thr}(AGU) gene in *Sc*Δ*thrS* to assess the ability of the human synthetase and tRNA to restore the growth phenotype. Under selective conditions, the combination of *TARS2*-Δ_N19 and hctRNA^{Thr}(AGU) rescued the growth of *Sc*Δ*thrS* (Fig. 2*E*), suggesting that hctRNA^{Thr}(AGU) was aminoacylated by hmtThrRS in yeast and could decode the corresponding codons *in vivo*. Under the same conditions, *TARS2*-Δ_N38 failed to support growth, despite the presence of overexpressed hctRNA^{Thr}(AGU) (Fig. 2*E*). Collectively, these data confirmed that the inability of hmtThrRS to replace *Sc*ThrRS *in vivo* is likely caused by its inability to charge *Sc*tRNA^{Thr}(AGU).

Amino Acid Activation Activity of hmtThrRS—Amino acid activation is the first step of tRNA aminoacylation, and the accurate selection of cognate amino acid activation by aaRS is indispensable for accurate protein synthesis. To date, various ThrRSs, including *E. coli* ThrRS (*Ec*ThrRS), *S. cerevisiae* ThrRS (*Sc*ThrRS), and *S. cerevisiae* mitochondrial ThrRS (*Sc*mtThrRS), have been reported to misactivate non-cognate Ser (19, 20, 22). On the other hand, several mitochondrial tRNA synthetases (such as LeuRS or PheRS) exhibit a stricter amino acid selection ability (23–25). To reveal the amino acid activation activity of hmtThrRS, we measured the activation kinetics of hmtThrRS for cognate Thr and non-cognate Ser and found that hmtThrRS has a much higher K_m value for Ser (180 ± 14 mM) compared with Thr (2.5 ± 0.1 mM) and that the k_{cat} value for Thr is 5-fold greater than that for Ser ((5.8 ± 0.2 s^{-1}) and (1.1 ± 0.02 s^{-1}), respectively) (Table 1). These data correspond to a discrimination factor of 383 in favor of Thr (Table 1); this is relatively low and not consistent with the overall *in vivo* rate of misincorporation during protein synthesis, which has been estimated to be in the range of 6×10^{-4} to 5×10^{-3}/amino acid incorporated (38, 39). In addition, the free Ser concentration slightly exceeds that of free Thr in mammalian mitochondria (1.81 and 1.33 nmol/mg of protein, respectively) (40), indicating that misactivation should be even higher *in vivo*. Altogether, these data showed that Ser might be misactivated by hmtThrRS *in vivo*, over the threat alert level for accurate decoding of Thr codons in human mitochondria. Low fidelity protein synthesis usually leads to increased amounts of unfolded proteins in the cells (6); therefore, it is likely that proofreading of the misactivated Ser would occur before and/or after its transfer onto tRNA^{Thr}.

Editing Properties of hmtThrRS—Usually one AMP molecule is formed per aminoacyl-tRNA produced during the aminoacylation reaction. In the presence of a non-cognate amino acid and a proofreading activity, the non-cognate adenylate or mischarged tRNA is hydrolyzed, releasing one AMP molecule per

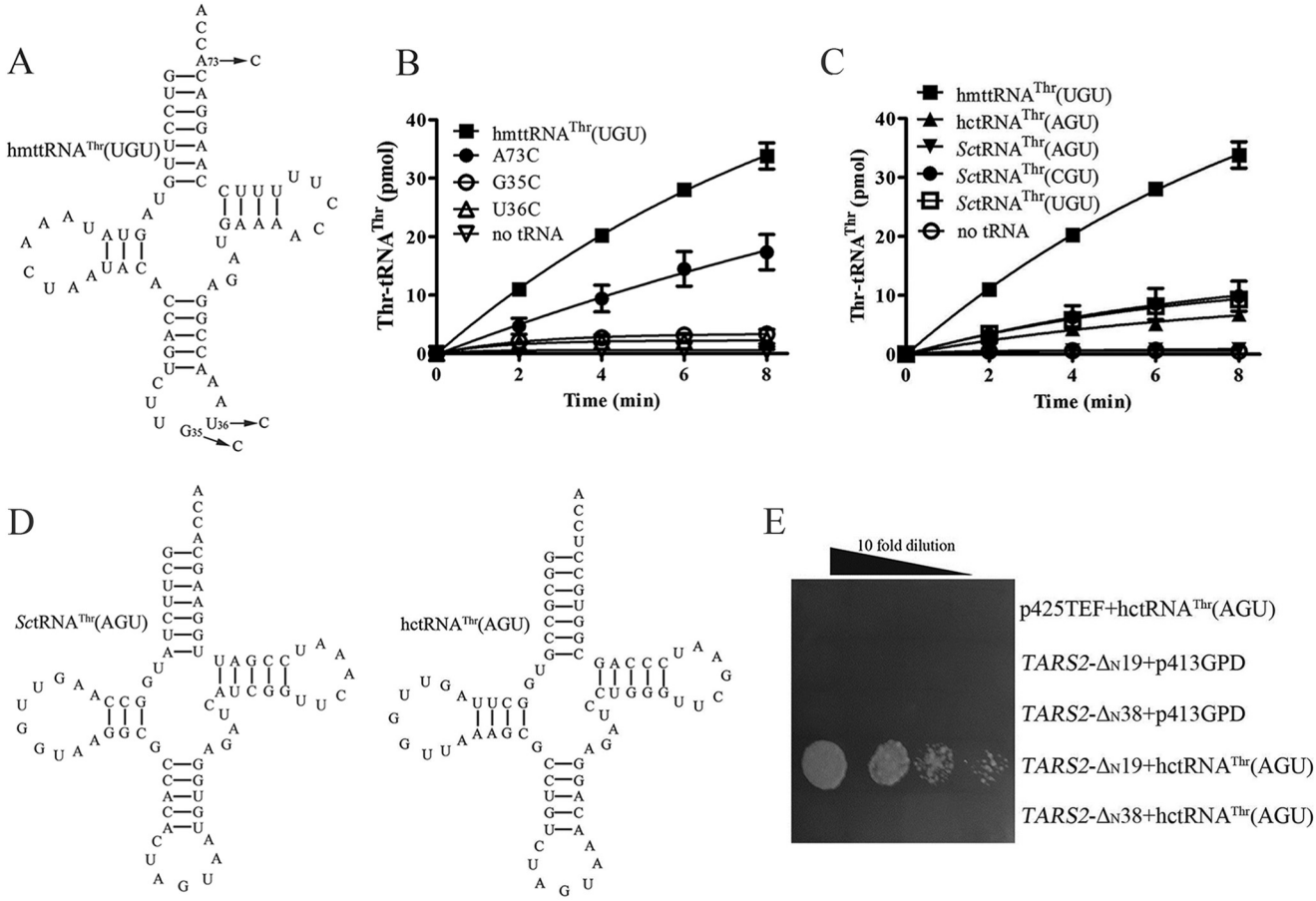

FIGURE 2. **hmttRNA^{Thr} determinants for aminoacylation and cross-species recognition of tRNA^{Thr} by hmtThrRS.** *A*, cloverleaf structure of hmttRNA^{Thr}(UGU) with mutations indicated. *B*, aminoacylation of hmttRNA^{Thr} and its mutants, including G35C, U36C, and A73C, by hmtThrRS. The control curve was obtained without tRNA addition. *C*, aminoacylation of hmttRNA^{Thr}(UGU), hctRNA^{Thr}(AGU), *Sc*tRNA^{Thr}(AGU), *Sc*tRNA^{Thr}(CGU), *Sc*tRNA^{Thr}(UGU), and control (without adding tRNA) by hmtThrRS. *D*, cloverleaf structures of *Sc*tRNA^{Thr}(AGU) and hctRNA^{Thr}(AGU). *E*, complementation phenotypes of hmtThrRS mutations with hctRNA^{Thr}(AGU). Drop test of *Sc*Δ*thrS* strain expressing hmtThrRS-Δ_N19 and hmtThrRS-Δ_N38 with hctRNA^{Thr}(AGU). Strains harboring empty p425TEF or empty p413GPD were used as negative controls. *Error bars*, S.D.

TABLE 1

Kinetic parameters of hmtThrRS for threonine and serine in the activation reaction as measured by an ATP-PP$_i$ exchange reaction

The results represent the average of three independent trials with the standard deviations indicated.

Amino acid	k_{cat}	K_m	k_{cat}/K_m	Discrimination factor
	s^{-1}	m_M	$m_M{}^{-1}s^{-1}$	
Thr	5.8 ± 0.2	2.5 ± 0.1	2.3	1
Ser	1.1 ± 0.02	180 ± 14	0.006	383

TABLE 2

k_{obs} of AMP formation of hmtThrRS and its variants in the presence of Ser

The results represent the average of three independent trials with the standard deviations indicated.

Enzyme	tRNA	k_{obs} ($\times 10^{-3}$)	Relative k_{obs}
		s^{-1}	%
hmtThrRS	+	18.9 ± 0.2	100
	−	3.5 ± 0.04	100
H133A/H137A	+	17.0 ± 0.2	90
	−	3.0 ± 0.3	86
P282L	+	2.8 ± 0.2	15
	−	1.1 ± 0.07	31

non-cognate amino acid activated or charged. The repetitive cycles of synthesis-hydrolysis of the non-cognate products consume more ATP and release proportional amounts of AMP, the quantification of which by TLC allows monitoring of the proofreading/editing activities. When performed in the presence of tRNA, the TLC assay measures all of the editing activities combined, including tRNA-independent and -dependent pretransfer editing, in addition to the post-transfer editing. In the absence of tRNA, the assay measures the AMP produced from the sole tRNA-independent pretransfer editing activity. With hmtThrRS and Ser as the non-cognate amino acid, in the absence or presence of hmttRNA^{Thr}, the observed rate value (k_{obs}) of AMP formation was (3.5 ± 0.04) × 10^{-3} s^{-1} and (18.9 ± 0.2) × 10^{-3} s^{-1}, respectively (Table 2 and Fig. 3*A*). Therefore, the AMP formation of hmtThrRS derives mainly from tRNA-dependent editing, which includes tRNA-dependent pretransfer and/or post-transfer editing. To identify the origin of the AMP formation, we inactivated the two critical His residues of the editing domain of ThrRS that are directly involved in post-transfer editing (20, 41). Based on sequence alignments, we constructed a double mutant targeting His^{133} and His^{137} of hmtThrRS (equivalents of His^{73} and His^{77} in *Ec*ThrRS) to obtain the double mutant hmtThrRS-H133A/H137A. In the TLC assay, it catalyzed AMP formation with k_{obs} values of (3.0 ± 0.3)×10^{-3} s^{-1} and (17.0 ± 0.2)×10^{-3} s^{-1} in

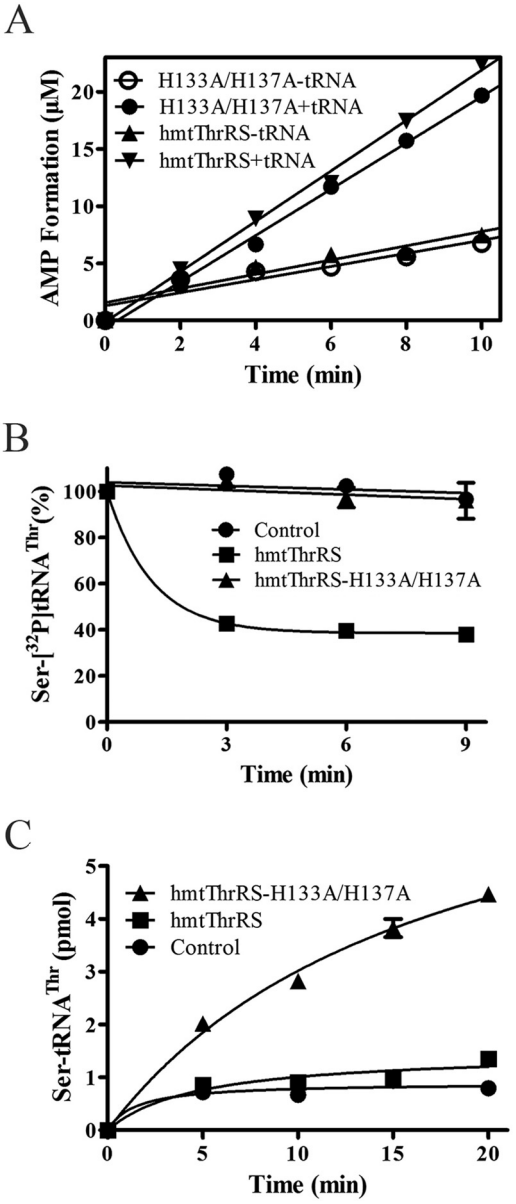

FIGURE 3. **Editing and mischarging properties of hmtThrRS and the mutated derivative hmtThrRS-H133A/H137A.** *A*, AMP formation by hmtThrRS and the double mutant in the presence of non-cognate Ser and in the presence or absence of tRNA. [^{32}P]AMP was quantified after TLC separation on PEI plates. *B*, deacylation of Ser-[^{32}P]hmttRNA^{Thr} by hmtThrRS and the double mutant hmtThrRS-H133A/H137A. The control without enzyme represents the spontaneous hydrolysis of mischarged tRNA. After incubation with ThrRS, the samples were treated by nuclease S1, and Ser-[^{32}P]AMP was quantified after TLC separation. *C*, mischarging of hmttRNAThr by [^{14}C]Ser catalyzed by hmtThrRS and the double mutant. The control curve was obtained without enzyme addition. *Error bars*, S.D.

the absence or presence of hmttRNA^{Thr}, respectively (Table 2 and Fig. 3*A*). Because the double mutant was supposed to be deprived of post-transfer activity, these nearly unchanged values suggested that the post-transfer editing only moderately contributes to total editing, whereas the majority of the AMP formed is derived from tRNA-dependent pretransfer editing. To confirm this deduction, we measured the deacylation activity of a preformed Ser-[^{32}P]tRNA^{Thr}. After nuclease S1 treatment, Ser-[^{32}P]AMP was separated from [^{32}P]AMP by TLC, and the deacylation activity was calculated. The assay showed that hmtThrRS has the capability to deacylate the mischarged tRNA, as expected from the post-transfer editing activity (Fig. 3*B*). However, deacylation of preformed Ser-tRNA^{Thr} showed that post-transfer editing of hmtThrRS-H133A/H137A is absent (Fig. 3*B*). Indeed, the mutant hmtThrRS-H133A/H137A formed much more Ser-tRNA^{Thr} than the wild-type hmtThrRS enzyme (Fig. 3*C*).

Thus, tRNA-independent pretransfer editing and post-transfer editing contribute little to the total editing, whereas majority of formed AMP is derived from tRNA-dependent pretransfer editing. However, post-transfer editing is the most efficient and critical safeguard to prevent Ser-tRNA^{Thr} synthesis, as demonstrated by its accumulation by hmtThrRS-H133A/H137A.

Analysis of Mitochondrial Disease-causing Pro to Leu Mutation at Position 282—Recently, a novel site mutant, P282L, in hmtThrRS was identified that potentially causes mitochondrial disease. Pro^{282} of the hmtThrRS precursor is absolutely conserved among eukaryotic ThrRS (Fig. 4*A*). In the bacterial *Ec*ThrRS structure (Protein Data Bank code 1QF6), the corresponding residue is located in a turn between the N2 editing domain and the peptide connecting the aminoacylation domain (Fig. 4*B*). Since Pro^{282} is located in such a crucial turn linking the N2 editing domain and the catalytic core, we speculated that, as a rigid amino acid, the contribution of Pro^{282} to the enzyme is to keep a proper conformation for the whole enzyme. Therefore, mutation of this key residue might change the protein structure and reduce its stability. We used various methods to assess the effect of the mutation on the protein's structure/stability. First, we compared the *in vivo* steady-state protein levels of FLAG-tagged wild-type hmtThrRS and hmtThrRS-P282L after overexpression in HEK293T cells. Western blot analysis using an anti-FLAG antibody showed that the protein level of hmtThrRS-P282L was only 36% of that of the wild-type enzyme (Fig. 4*C*). Such a reduction might result from a decrease in protein synthesis or faster degradation. However, the point mutation only changes a CCC Pro codon to a CUC Leu codon, both codons being frequently used in humans. Therefore, the decrease in the steady-state level of the P282L protein was more likely to result from faster degradation related to its stability. Consequently, we focused our investigations on the analysis of the protein structure and stability. After purification of hmtThrRS-P282L, we performed a CD analysis of native hmtThrRS and hmtThrRS-P282L. The CD spectrum of wild-type ThrRS was characteristic of an α-helical protein with negative bands at 222 and 208 nm and a positive band at 193 nm (42). However, the spectrum from the P282L mutant was slightly different, with a shift of the 222 and 208 nm peaks toward shorter wavelengths, suggesting structural differences between the two proteins (Fig. 4*D*). In addition, assuming that such a structural change would affect the binding of a substrate with an extended binding site, such as tRNA^{Thr}, we measured and compared the dissociation constant (K_D) of two proteins for hmttRNA^{Thr} using a filter binding assay (33, 34). Surprisingly, the K_D value of the P282L mutant was decreased compared with that of the native enzyme (0.50 $\pm$ 0.04 and 1.83 $\pm$ 0.13 μM, respectively) (Fig. 4, *E* and *F*), indicating that the mutant binds tRNA^{Thr} more tightly. Finally, we measured the thermal stability of hmt-

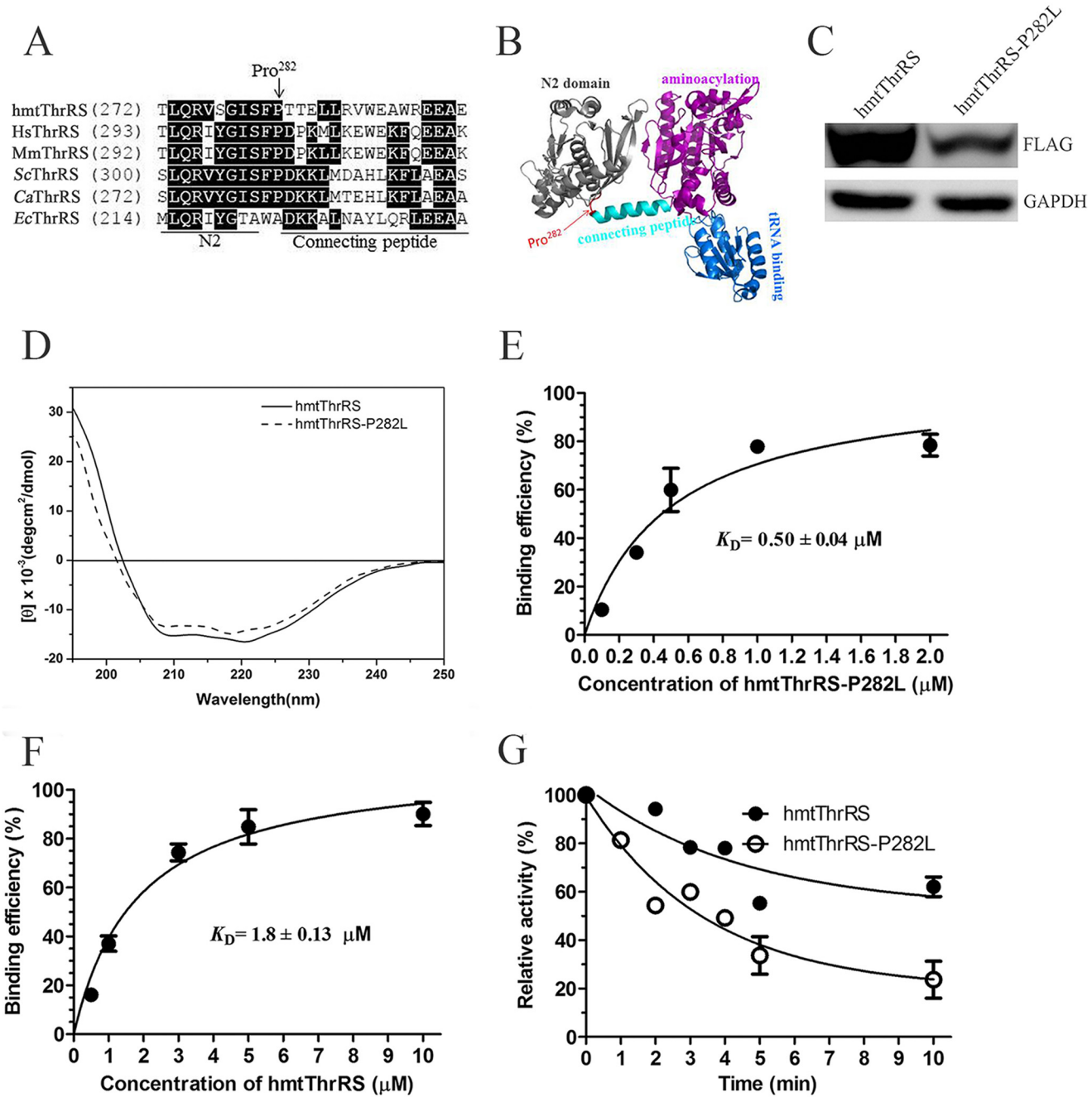

FIGURE 4. **Analyses of the structure and stability of hmtThrRS-P282L.** *A*, sequence alignment of different ThrRS with the position of amino acid 282 indicated. *Hs*, *Homo sapiens*; *Mm*, *Mus musculus*; *Sc*, *Saccharomyces cerevisiae*; *Ca*, *Candida albicans*; *Ec*, *Escherichia coli*. *B*, putative location of Pro^{282} in hmtThrRS. The *arrow* shows the corresponding residue in the *Ec*ThrRS crystallographic structure (Protein Data Bank code 1QF6). *C*, measurements of protein levels of hmtThrRS and hmtThrRS-P282L by Western blotting after overexpression in HEK293T cells. GAPDH was used as the internal control. *D*, CD analysis of hmtThrRS and hmtThrRS-P282L. The CD spectra of the two proteins are presented as molar residue ellipticity (deg.cm^{2}dmol^{-1}). *E* and *F*, measurement of equilibrium dissociation constants for hmtThrRS-P282L (*E*) and hmtThrRS (*F*) by filter binding assays. *G*, comparison of the thermal resistance of hmtThrRS and hmtThrRS-P282L. Aminoacylation activities were measured after increasing incubation times of heating at 50 °C. Activities were represented as a percentage of the initial activity before heating. *Error bars*, S.D.

ThrRS and hmtThrRS-P282L after heating at 50 °C. After various incubation times, the residual activity was measured at 37 °C. Whereas the half-life (50% of residual activity) of the native enzyme was greater than 10 min, the half-life of the mutant was only 3.25 min, suggesting that the mutant was more unstable at 50 °C than the wild-type enzyme (Fig. 4*G*). Taken together, these data indicated strongly that mutation of the conserved Pro^{282}, located between the two domains, alters the structure and stability of hmtThrRS.

We further analyzed whether the structural alteration affected amino acid activation, aminoacylation, and editing capacities. Kinetic parameters in the ATP-PP$_i$ exchange reaction showed that the catalytic efficiency (k_{cat}/K_m) of Thr activation was only 61% of that of hmtThrRS, caused by an increase in K_m and a decrease in k_{cat} (Table 3). Further aminoacylation kinetic analysis showed that the k_{cat} of the mutant was decreased compared with that of hmtThrRS. The K_m for tRNA was increased 2-fold, and the resulting catalytic efficiency (k_{cat}/

TABLE 3

Kinetic parameters of hmtThrRS and hmtThrRS-P282L for Thr in the activation reaction, as measured in the ATP-PP_i exchange reaction

The results represent the average of three independent trials with the standard deviations indicated.

Enzyme	k_{cat}	K_m	k_{cat}/K_m	Relative k_{cat}/K_m
	s^{-1}	m_M	$m_M^{-1}s^{-1}$	%
hmtThrRS	5.8 ± 0.2	2.5 ± 0.1	2.3	100
P282L	4.4 ± 0.3	3.1 ± 0.3	1.4	61

TABLE 4

Aminoacylation kinetics of hmtThrRS and hmtThrRS-P282L for $tRNA^{Thr}$

The results represent the average of three independent trials with the standard deviations indicated.

Enzyme	k_{cat}	K_m	k_{cat}/K_m ($\times 10^{-3}$)	Relative k_{cat}/K_m
	s^{-1}	μ_M	$\mu_M^{-1}s^{-1}$	%
hmtThrRS	0.061 ± 0.002	1.1 ± 0.03	55	100
P282L	0.015 ± 0.005	2.0 ± 0.2	7.5	13

K_m) was only 13% of that of native enzyme (Table 4). Thus, our data clearly revealed that both amino acid activation and tRNA charging are negatively affected by the mutation. To further determine whether the residual aminoacylation activity could support protein translation *in vivo*, we simultaneously introduced p425TEF-hmtThrRS-P282L and p413GPD-hc $tRNA^{Thr}$(AGU) into strain *Sc*Δ*thrS* and observed its growth phenotype on 5-FOA-containing selective medium. No growth difference was detected when comparing the yeast clones expressing native hmtThrRS and hmtThrRS-P282L (Fig. 5*A*), indicating that partial loss of function did not affect global protein synthesis critically. This is consistent with our previous study, which showed that an *Sc*ThrRS mutant with only 5% aminoacylation activity was able to sustain protein synthesis *in vivo* (36). Pro^{310} of *Sc*ThrRS is equivalent to Pro^{282} of hmtThrRS. To test the effect of the mutation on *Sc*ThrRS, we constructed *Sc*ThrRS-P310L. A complementation assay in yeast strain *Sc*Δ*thrS* was then performed after introducing either the *Sc*ThrRS or *Sc*ThrRS-P310L genes. The results showed that *Sc*ThrRS-P310L was able to support yeast growth as efficiently as native *Sc*ThrRS (Fig. 5*B*). However, Western blot analysis with an antibody targeting the C-terminal His_6 tag revealed that the steady-state level of *Sc*ThrRS-P310L was ~25% of that of the native *Sc*ThrRS (Fig. 5*C*). This result was consistent with the relative protein level of hmtThrRS and hmtThrRS-P282L in HEK293T cells (Fig. 4*C*) and confirmed the important role of this conserved Pro in the subtle structure and/or stability of the enzyme.

In addition to the effects on amino acid activation and aminoacylation, the P282L mutation may also affect the proofreading activities of hmtThrRS, which is essential to clear misactivated Ser or mischarged Ser-$tRNA^{Thr}$. Indeed, a decrease in the translational quality control mechanism is another potential factor leading to cellular dysfunctions or disorders (43). We carried out AMP formation assays in the presence of non-cognate Ser to measure the total editing activity of hmtThrRS. The data showed that both tRNA-independent pretransfer editing and the total editing activity of the mutant were decreased to 15% of wild-type enzyme values (Table 2 and Fig. 5*D*), whereas the post-transfer editing, as measured in the deacylation assay of Ser-$tRNA^{Thr}$, was negligibly affected (Fig. 5*E*). Collectively, the data suggested that the replacement of Pro with Leu at position 282 of hmtThrRS alters the structure and/or stability of the enzyme, which in turn has a negative effect on its activities of amino acid activation, tRNA aminoacylation, and proofreading.

Identification of an Alternative Splice Variant of TARS2—During the process of cloning of *TARS2* from HEK293T cells, a cDNA library was generated by reverse transcription with an oligo(dT) primer. After PCR amplification of the cDNA, two forms of *TARS2* were cloned, one being shorter than the expected size (Fig. 6*A*). DNA sequencing revealed that the shorter isoform lacks 246 nucleotides compared with the wild-type *TARS2* mRNA. Deletion of the 246-nt (encoding a peptide ranging from Asn^{259} to Arg^{340} of hmtThrRS) does not alter the downstream reading frame. By sequence alignment and structure comparison with *Ec*ThrRS, we found that the deletion removes part of the N2 editing domain, the aminoacylation domain, and the peptide linker connecting the two domains (data not shown) (17). Analysis of the intron and exon sequences revealed that this isoform could be derived from alternative splicing that skipped exons 8 and 9, ligating exon 7 to 10 directly (Fig. 6*B*). This in-frame splicing variant was named hmtThrRS-SV to distinguish it from native hmtThrRS. To explore whether hmtThrRS-SV mRNA is present in other cell types, we designed two primers spanning exon 7 to exon 10 to amplify this region from cDNA libraries of five human cell lines. Both native hmtThrRS and hmtThrRS-SV mRNA were found in these cell lines (Fig. 6*C*). The relative abundance of the native and splicing variant mRNAs was measured by qPCR in each cDNA sample (Fig. 6*D*). Two primer sets, one pair specific to the native mRNA spanning exon 8 and exon 9 and the other to the splicing variant mRNAs of the exon 7/10 boundaries, were used. We optimized the qPCR reactions to produce specific DNA fragments with high efficiency. The splicing variant was present in all tested cell lines in proportions ranging between 40 and 26%, with the highest level in BEAS-2B cells (40%) and the lowest level in Jurkat cells (26%) (Fig. 6*D*).

To determine whether the predicted product of hmtThrRS-SV can fold into a stable protein *in vivo*, we constructed a plasmid harboring hmtThrRS-SV (pCMV-3Tag-3A-hmtThrRS-SV precursor). After transfection into HEK293T cells, it generated a soluble protein with the predicted size (Fig. 6*E*); however, the amount of hmtThrRS-SV was lower than that of the wild-type hmtThrRS.

hmtThrRS-SV Is Targeted into Mitochondria but Fails to Form Homodimers—The mRNA sequence for hmtThrRS-SV has the normal initiation codon at the beginning of the MTS; therefore, we checked whether hmtThrRS-SV could be detected in mitochondria. To this end, the genes of hmtThrRS and hmtThrRS-SV were expressed in HEK293T cells, and their intracellular localizations were observed by confocal microscopy using MitoTracker staining as a mitochondrial marker. As expected, the wild-type hmtThrRS is transported into the mitochondria and co-localizes with the MitoTracker staining (Fig. 7*A*). Similarly, hmtThrRS-SV co-localizes with the immunofluorescence of MitoTracker, however with a more dispersed,

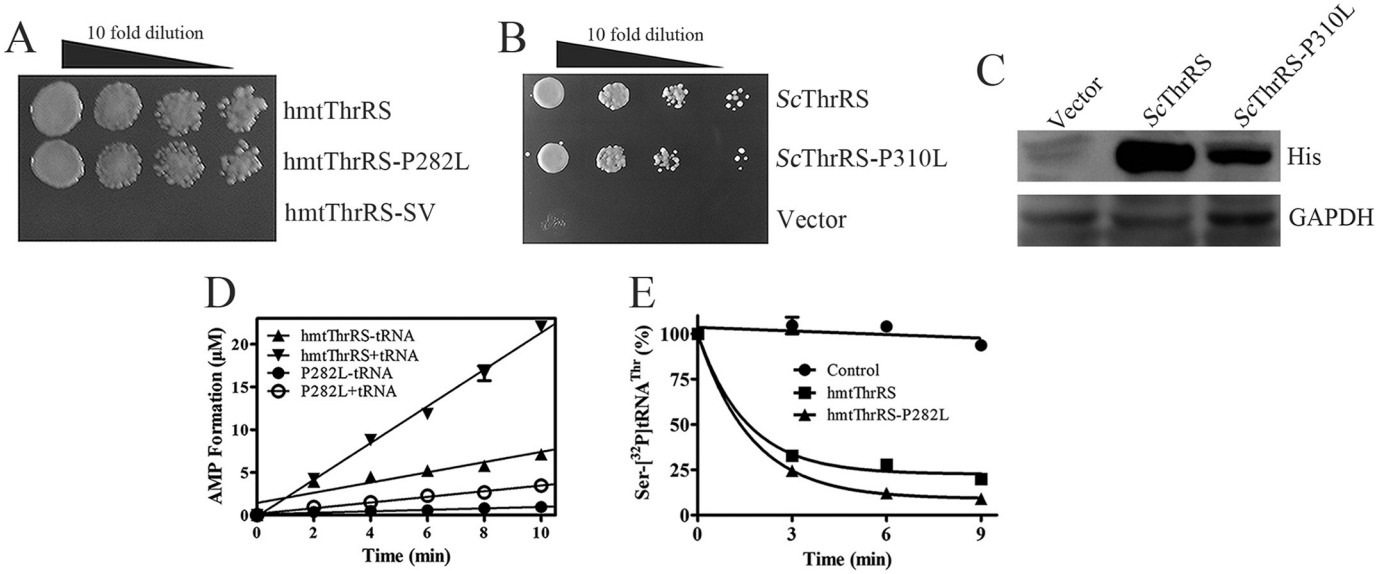

FIGURE 5. **Editing properties and *in vivo* activity of hmtThrRS-P282L.** *A*, complementation phenotypes of hmtThrRS and its mutations with hctRNA^{Thr}(AGU). Drop test shows *Sc*Δ*thrS* strains expressing hmtThrRS, hmtThrRS-P282L, and hmtThrRS-SV with hctRNA^{Thr}(AGU). *B*, complementation phenotypes of *Sc*ThrRS and *Sc*ThrRS-P310L. *C*, detection of the amounts of *Sc*ThrRS and *Sc*ThrRS-P310L by Western blotting. GAPDH was used as the internal control. *D*, quantification of AMP formation in the presence of non-cognate Ser by hmtThrRS with or without tRNA or by hmtThrRS-P282L with or without tRNA. *E*, deacylation of Ser-[^{32}P]hmttRNA^{Thr} by hmtThrRS and hmtThrRS-P282L and the control without the addition of enzyme. *Error bars*, S.D.

punctuated pattern of fluorescence (Fig. 7*A*). These results confirmed that hmtThrRS-SV is targeted to the mitochondria and might participate in mitochondrial function. Therefore, we checked whether the splicing variant could form dimers. To this end, different combinations of genes of FLAG- and c-Myc-tagged hmtThrRS or hmtThrRS-SV were co-expressed in HEK293T cells. Cell lysates were immunoprecipitated with anti-FLAG antibodies. Western blotting showed that c-Myc-tagged hmtThrRS was co-immunoprecipitated by the anti-FLAG antibody (Fig. 7*B*), suggesting that the c-Myc-hmtThrRS and FLAG-hmtThrRS subunits could form homodimers, as expected. By contrast, c-Myc-tagged hmtThrRS-SV could not be co-immunoprecipitated by the anti-FLAG antibody, although FLAG-hmtThrRS-SV was well immunoprecipitated by the anti-FLAG antibody (Fig. 7*B*). This result showed that hmtThrRS-SV is unable to dimerize *in vivo*.

Recently, we reported that dimerization is essential for yeast ThrRS to catalyze the aminoacylation reaction (36). Therefore, we checked whether the hmtThrRS-SV, which is unable to dimerize, is similarly inactive. Because hmtThrRS-SV was detected in HEK293 cells (Fig. 6*E*), this suggested that an *in vivo* assay would be a suitable way to assess its activity. Consequently, hmtThrRS-SV and hctRNA^{Thr}(AGU) were expressed in yeast knock-out strain *Sc*Δ*thrS*, and complementation assays were performed in the presence of the selective compound 5-FOA. Unfortunately, hmtThrRS-SV failed to support the growth of yeast transformants, indicating that hmtThrRS-SV is inactive *in vivo* (Fig. 5*A*). In parallel, we deleted the corresponding peptide (Asn^{287} to Arg^{368}) from yeast *Sc*ThrRS to produce a protein mimicking the splicing variant, named *Sc*ThrRS-SV. *In vivo* complementation assays showed that *Sc*ThrRS-SV similarly failed to rescue the loss of the *Sc*ThrRS gene (Fig. 7*C*). This result confirmed that deletion of this peptide corresponding to exons 8–9 impairs the function of ThrRS by a catalytic and/or structural effect (dimerization or incorrect folding).

Discussion

Human Mitochondrial ThrRS Misactivates Ser and Mainly Uses tRNA-dependent Editing to Prevent Synthesis of Ser-tRNA^{Thr}—For several aaRSs, including class I LeuRS, IleRS, and ValRS and class II ProRS, PheRS, ThrRS, and AlaRS, the editing activity is an essential requisite to ensure accurate tRNA aminoacylation (4). This seems to be conserved in many bacterial, archaeal, and eukaryotic cytoplasmic synthetases; however, little is known about the editing of aaRS from mitochondria. The restricted metabolic processes occurring in the mitochondria suggest that fewer competing metabolites and amino acids are present in this compartment. However, surprisingly, it appears that mitochondrial aaRS are more specific for their cognate amino acids. This is the case for human mitochondrial LeuRS, which can precisely discriminate Leu from non-cognate Ile thanks to its more accurate amino acid binding pocket. This makes the rejection of Ile at the editing step unnecessary, and indeed, catalytic residues of the editing site have been lost in addition to the editing activity (23). Similarly, yeast mitochondrial PheRS lacks an editing domain but is extremely specific for the generation of Phe-tRNA^{Phe} (24, 25).

Considering the editing of ThrRS, it has been reported that bacterial ThrRS uses post-transfer editing to remove Ser-tRNA^{Thr} (41) and eukaryotic cytoplasmic ThrRS uses tRNA-independent and -dependent pretransfer editing and post-transfer editing to prevent Ser mischarging (20). Most archaeal ThrRS possess an editing domain homologous to D-tyrosyl-tRNA^{Tyr} deacylases (44). However, several cases of archaeal ThrRS lacking an editing domain also have been reported, and a trans-editing factor, containing an anticodon-binding domain, is used to prevent formation of mischarged tRNA^{Thr} (45). On the other hand, *Sc*mtThrRS, which naturally lacks the editing domain, only exhibits pretransfer editing to hydrolyze non-cognate Ser adenylate (22). This editing process is incomplete,

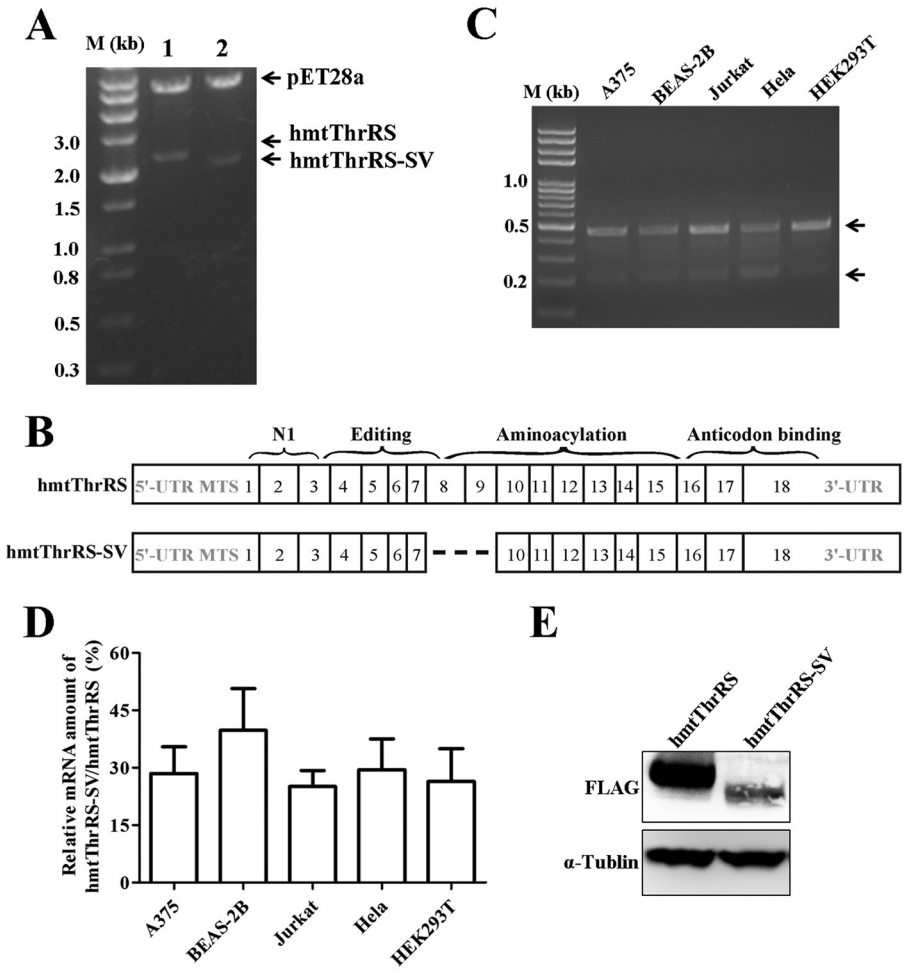

FIGURE 6. **Detection of a splicing variant of *TARS2* in different cell lines.** *A*, cloning of *TARS2* cDNA led to two different plasmid constructs. DNA sequencing revealed the whole sequence of native hmtThrRS (*lane 1*) and a truncated sequence lacking 246 nucleotides of exons 8 and 9, termed hmtThrRS-SV (*lane 2*). *B*, schematic representation of the exon composition of hmtThrRS and hmtThrRS-SV. The domain structure of both proteins is also indicated at the *top*. *C*, detection of the hmtThrRS-SV in different cell lines. PCR amplification with oligonucleotides pairing with exon 7 (forward) and exon 10 (reverse) shows that the native (*upper bands*) and splice variant hmtThrRS (*lower bands*) co-exist in five different human cell lines. *D*, relative amounts of hmtThrRS-SV mRNA to hmtThrRS mRNA in different cell lines. qPCR experiments were performed with one set of primers spanning exons 8 and 9 (detecting the native hmtThrRS) and the other recognizing the exon 7 to 10 boundary (detecting the hmtThrRS-SV). qPCR values obtained for each cell line were normalized to GAPDH mRNA levels. Relative mRNA levels of hmtThrRS-SV were calculated using ΔΔCt method based on three independent qPCR assays. *Error bars*, S.D. *E*, Western blotting detection of the native full-length hmtThrRS and truncated hmtThrRS corresponding to the splice variant mRNA. Full-length hmtThrRS and hmtThrRS-SV were cloned in pCMV-3Tag-3A, and HEK293T cells were transfected.

and Ser-tRNA^{Thr} is produced *in vitro* by *Sc*mtThrRS, which raises the question of the threshold of mischarging endured by the cell (22).

Here, we showed that hmtThrRS does not exhibit an especially specific active site, such as *Sc*mtPheRS or hmtLeuRS, and it significantly misactivates Ser. In return, it exhibits tRNA-independent and tRNA-dependent pretransfer editing, and post-transfer editing activities, to hydrolyze Ser-AMP and Ser-tRNA^{Thr}. This may explain why hmtThrRS has an intact editing domain, whereas hmtLeuRS exhibits an inactive one. As reported for *Sc*ThrRS (20), we found that post-transfer editing of hmtThrRS was the most efficient way to prevent Ser-tRNA^{Thr} synthesis, although it contributed little to the total editing.

Mutation Causing Human Mitochondrial Encephalomyopathies Affects Protein Structure/Stability and Enzymatic Activities of ThrRS—Recently, a mutation of Pro to Leu at position 282 of hmtThrRS was identified in a patient presenting mitochondrial disorders (26). Despite decreased levels of protein and charged tRNA^{Thr}, the molecular consequence of the mutation could not be understood (26). Here, we compared the activities of the mutant to native hmtThrRS in the amino acid activation, tRNA charging, and editing reactions. All activities were obviously influenced by the mutation. In addition, using a *Sc*ThrRS gene deletion strain and analyzing steady-state protein levels, we revealed that this conserved residue also regulates steady-state protein level *in vivo*, which is reasonable, because Pro residues in proteins are often located at key conformational positions. Indeed, Pro^{282} of hmtThrRS is a well conserved site in all eukaryotic ThrRS, and is located in a crucial turn region linking the end of the N2 editing domain and a connecting peptide to the aminoacylation domain. Our data from various analyses suggested that the P282L mutation negatively alters the structure and/or influences protein stability, possibly by affecting the global orientation of the domain or the protein. However, because Pro^{282} is distant from both aminoacylation and editing active sites, and has no potential interac-

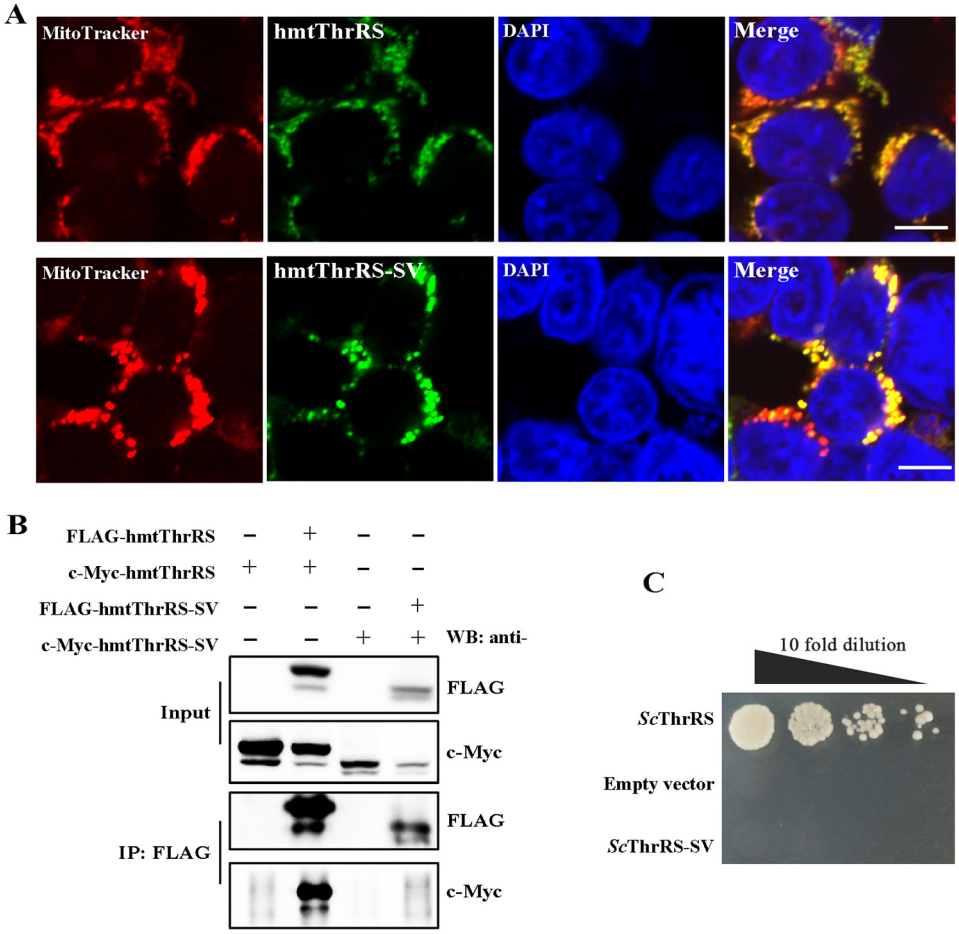

FIGURE 7. **Mitochondrial import of hmtThrRS-SV and *in vivo* structural and functional properties.** *A*, both native hmtThrRS and hmtThrRS-SV localized in the mitochondria. HEK293T cells were transfected with the FLAG-tagged constructs of pCMV-3Tag-3A containing the coding sequences for native hmtThrRS or hmtThrRS-SV, respectively. The cells were stained with MitoTracker and immunostained with anti-FLAG. Fluorescent images of MitoTracker (*red*) and FLAG (*green*) and the nuclear counterstain DAPI (*blue*) were captured by a confocal microscope. *Scale*, 20 μm. *B*, HEK293T cells were co-transfected with pCMV-3Tag-4A-hmtThrRS (c-Myc-tagged hmtThrRS) in the presence of pCMV-3Tag-3A-hmtThrRS (FLAG-tagged hmtThrRS) or control vector pCMV-3Tag-3A. The same procedures were performed for hmtThrRS-SV. Cell lysates were immunoprecipitated with anti-FLAG antibodies conjugated to agarose beads. Western blotting was used to detect whether c-Myc-tagged proteins were co-immunoprecipitated with FLAG-tagged proteins. *C*, a shuffle assay showing that the *Sc*ThrRS-SV could not complement the *Sc*Δ*thrS* strain. Wild-type *Sc*ThrRS and empty vector p425TEF were used as controls.

tion with $tRNA^{Thr}$ (as deduced from the *Ec*ThrRS-$tRNA^{Thr}$ structure (Protein Data Bank code 1QF6), we proposed that the decreased activity of the mutant is a secondary effect of alterations in protein conformation.

Existence of an Alternative Splicing Variant with Possible Non-translational Function—Recently, it was reported that nearly all aaRS genes in humans encode multiple splicing variants, creating a large number of aaRS-related catalytic nulls (28). These catalytic nulls usually keep their non-catalytic domains and exhibit deletions or truncations in the catalytic core, inducing loss of tRNA aminoacylation activity. Although some of these proteins have been detected in cell extracts by Western blotting, their physiological functions remain to be determined. Here, we identified a *TARS2* splicing variant in several human cell lines, which encodes a hmtThrRS derivative lacking a peptide covering a portion of both the editing and the aminoacylation domains. Our data revealed that this mutant is unable to dimerize and cannot complement a yeast strain deleted for the ThrRS gene, suggesting that it is deficient in catalyzing Thr-$tRNA^{Thr}$ formation for protein synthesis. Meanwhile, we found that the protein could not be purified and it formed inclusion bodies in *E. coli* (data not shown), because skipping exon 8 and 9 causes a drastic protein deletion, which affects the N2 editing domain, catalytic core, and dimer interface with putative effects on protein dimerization (data not shown) (17). The data also showed that the splicing variant is readily translated and imported into mitochondria. It has been shown that mitochondria may contain aaRS-like proteins that play crucial roles in mitochondria metabolism. For example, a seryl-tRNA synthetase-like protein is found in mitochondria from insects, the deletion of which causes alterations in mitochondrial structure, function, and biogenesis without connection to $tRNA^{Ser}$ aminoacylation (46). Similarly, the catalytically inactive splicing variant of ThrRS identified here may have some non-canonical function besides $tRNA^{Thr}$ aminoacylation, and this needs to be explored functionally.

Author Contributions—Y. W., X. L. Z., and Z. R. R. performed the experiments. R. J. L. analyzed protein structure. G. E. analyzed the data. X. L. Z. and E. D. W. designed the experiments, analyzed the data, and wrote the paper.

References

1. Ibba, M., and Soll, D. (2000) Aminoacyl-tRNA synthesis. *Annu. Rev. Biochem.* **69,** 617–650
2. Schimmel, P. (1987) Aminoacyl tRNA synthetases: general scheme of structure-function relationships in the polypeptides and recognition of transfer RNAs. *Annu. Rev. Biochem.* **56,** 125–158
3. Loftfield, R. B., and Vanderjagt, D. (1972) The frequency of errors in protein biosynthesis. *Biochem. J.* **128,** 1353–1356
4. Zhou, X., and Wang, E. (2013) Transfer RNA: a dancer between charging and mis-charging for protein biosynthesis. *Sci. China Life Sci.* **56,** 921–932
5. Lee, J. W., Beebe, K., Nangle, L. A., Jang, J., Longo-Guess, C. M., Cook, S. A., Davisson, M. T., Sundberg, J. P., Schimmel, P., and Ackerman, S. L. (2006) Editing-defective tRNA synthetase causes protein misfolding and neurodegeneration. *Nature* **443,** 50–55
6. Nangle, L. A., De Crecy Lagard, V., Doring, V., and Schimmel, P. (2002) Genetic code ambiguity. Cell viability related to the severity of editing defects in mutant tRNA synthetases. *J. Biol. Chem.* **277,** 45729–45733
7. Zhou, X. L., Du, D. H., Tan, M., Lei, H. Y., Ruan, L. L., Eriani, G., and Wang, E. D. (2011) Role of tRNA amino acid-accepting end in aminoacylation and its quality control. *Nucleic Acids Res.* **39,** 8857–8868
8. Nangle, L. A., Motta, C. M., and Schimmel, P. (2006) Global effects of mistranslation from an editing defect in mammalian cells. *Chem. Biol.* **13,** 1091–1100
9. Newmeyer, D. D., and Ferguson-Miller, S. (2003) Mitochondria: releasing power for life and unleashing the machineries of death. *Cell* **112,** 481–490
10. Anderson, S., Bankier, A. T., Barrell, B. G., de Bruijn, M. H., Coulson, A. R., Drouin, J., Eperon, I. C., Nierlich, D. P., Roe, B. A., Sanger, F., Schreier, P. H., Smith, A. J., Staden, R., and Young, I. G. (1981) Sequence and organization of the human mitochondrial genome. *Nature* **290,** 457–465
11. Ojala, D., Montoya, J., and Attardi, G. (1981) tRNA punctuation model of RNA processing in human mitochondria. *Nature* **290,** 470–474
12. Allen, J. F., and Raven, J. A. (1996) Free-radical-induced mutation vs redox regulation: costs and benefits of genes in organelles. *J. Mol. Evol.* **42,** 482–492
13. Pesole, G., Gissi, C., De Chirico, A., and Saccone, C. (1999) Nucleotide substitution rate of mammalian mitochondrial genomes. *J. Mol. Evol.* **48,** 427–434
14. Scaglia, F., and Wong, L. J. (2008) Human mitochondrial transfer RNAs: role of pathogenic mutation in disease. *Muscle Nerve* **37,** 150–171
15. Florentz, C., Sohm, B., Tryoen-Tóth, P., Pütz, J., and Sissler, M. (2003) Human mitochondrial tRNAs in health and disease. *Cell. Mol. Life Sci.* **60,** 1356–1375
16. Scheper, G. C., van der Klok, T., van Andel, R. J., van Berkel, C. G., Sissler, M., Smet, J., Muravina, T. I., Serkov, S. V., Uziel, G., Bugiani, M., Schiffmann, R., Krägeloh-Mann, I., Smeitink, J. A., Florentz, C., Van Coster, R., Pronk, J. C., and van der Knaap, M. S. (2007) Mitochondrial aspartyl-tRNA synthetase deficiency causes leukoencephalopathy with brain stem and spinal cord involvement and lactate elevation. *Nat. Genet.* **39,** 534–539
17. Sankaranarayanan, R., Dock-Bregeon, A. C., Romby, P., Caillet, J., Springer, M., Rees, B., Ehresmann, C., Ehresmann, B., and Moras, D. (1999) The structure of threonyl-tRNA synthetase-tRNA(Thr) complex enlightens its repressor activity and reveals an essential zinc ion in the active site. *Cell* **97,** 371–381
18. Minajigi, A., and Francklyn, C. S. (2010) Aminoacyl transfer rate dictates choice of editing pathway in threonyl-tRNA synthetase. *J. Biol. Chem.* **285,** 23810–23817
19. Dock-Bregeon, A., Sankaranarayanan, R., Romby, P., Caillet, J., Springer, M., Rees, B., Francklyn, C. S., Ehresmann, C., and Moras, D. (2000) Transfer RNA-mediated editing in threonyl-tRNA synthetase: the class II solution to the double discrimination problem. *Cell* **103,** 877–884
20. Zhou, X. L., Ruan, Z. R., Huang, Q., Tan, M., and Wang, E. D. (2013) Translational fidelity maintenance preventing Ser mis-incorporation at Thr codon in protein from eukaryote. *Nucleic Acids Res.* **41,** 302–314
21. Ling, J., Peterson, K. M., Simonović, I., Cho, C., Söll, D., and Simonović, M. (2012) Yeast mitochondrial threonyl-tRNA synthetase recognizes tRNA isoacceptors by distinct mechanisms and promotes CUN codon reassignment. *Proc. Natl. Acad. Sci. U.S.A.* **109,** 3281–3286
22. Zhou, X. L., Ruan, Z. R., Wang, M., Fang, Z. P., Wang, Y., Chen, Y., Liu, R. J., Eriani, G., and Wang, E. D. (2014) A minimalist mitochondrial threonyl-tRNA synthetase exhibits tRNA-isoacceptor specificity during proofreading. *Nucleic Acids Res.* **42,** 13873–13886
23. Lue, S. W., and Kelley, S. O. (2005) An aminoacyl-tRNA synthetase with a defunct editing site. *Biochemistry* **44,** 3010–3016
24. Reynolds, N. M., Ling, J., Roy, H., Banerjee, R., Repasky, S. E., Hamel, P., and Ibba, M. (2010) Cell-specific differences in the requirements for translation quality control. *Proc. Natl. Acad. Sci. U.S.A.* **107,** 4063–4068
25. Roy, H., Ling, J., Alfonzo, J., and Ibba, M. (2005) Loss of editing activity during the evolution of mitochondrial phenylalanyl-tRNA synthetase. *J. Biol. Chem.* **280,** 38186–38192
26. Diodato, D., Melchionda, L., Haack, T. B., Dallabona, C., Baruffini, E., Donnini, C., Granata, T., Ragona, F., Balestri, P., Margollicci, M., Lamantea, E., Nasca, A., Powell, C. A., Minczuk, M., Strom, T. M., Meitinger, T., Prokisch, H., Lamperti, C., Zeviani, M., and Ghezzi, D. (2014) VARS2 and TARS2 mutations in patients with mitochondrial encephalomyopathies. *Hum. Mutat.* **35,** 983–989
27. Guo, M., Schimmel, P., and Yang, X. L. (2010) Functional expansion of human tRNA synthetases achieved by structural inventions. *FEBS Lett.* **584,** 434–442
28. Lo, W. S., Gardiner, E., Xu, Z., Lau, C. F., Wang, F., Zhou, J. J., Mendlein, J. D., Nangle, L. A., Chiang, K. P., Yang, X. L., Au, K. F., Wong, W. H., Guo, M., Zhang, M., and Schimmel, P. (2014) Human tRNA synthetase catalytic nulls with diverse functions. *Science* **345,** 328–332
29. Zhou, X. L., Zhu, B., and Wang, E. D. (2008) The CP2 domain of leucyl-tRNA synthetase is crucial for amino acid activation and post-transfer editing. *J. Biol. Chem.* **283,** 36608–36616
30. Jazwinski, S. M. (1990) Preparation of extracts from yeast. *Methods Enzymol.* **182,** 154–174
31. Livak, K. J., and Schmittgen, T. D. (2001) Analysis of relative gene expression data using real-time quantitative PCR and the 2(-ΔΔC(T)) method. *Methods* **25,** 402–408
32. Ling, C., Yao, Y. N., Zheng, Y. G., Wei, H., Wang, L., Wu, X. F., and Wang, E. D. (2005) The C-terminal appended domain of human cytosolic leucyl-tRNA synthetase is indispensable in its interaction with arginyl-tRNA synthetase in the multi-tRNA synthetase complex. *J. Biol. Chem.* **280,** 34755–34763
33. Yarus, M., and Berg, P. (1970) On the properties and utility of a membrane filter assay in the study of isoleucyl-tRNA synthetase. *Anal. Biochem.* **35,** 450–465
34. Michel, S. L., Guerrerio, A. L., and Berg, J. M. (2003) Selective RNA binding by a single CCCH zinc-binding domain from Nup475 (tristetraprolin). *Biochemistry* **42,** 4626–4630
35. Bonnefond, L., Fender, A., Rudinger-Thirion, J., Giegé, R., Florentz, C., and Sissler, M. (2005) Toward the full set of human mitochondrial aminoacyl-tRNA synthetases: characterization of AspRS and TyrRS. *Biochemistry* **44,** 4805–4816
36. Ruan, Z. R., Fang, Z. P., Ye, Q., Lei, H. Y., Eriani, G., Zhou, X. L., and Wang, E. D. (2015) Identification of lethal mutations in yeast threonyl-tRNA synthetase revealing critical residues in its human homolog. *J. Biol. Chem.* **290,** 1664–1678
37. Nameki, N. (1995) Identity elements of tRNA(Thr) towards *Saccharomyces cerevisiae* threonyl-tRNA synthetase. *Nucleic Acids Res.* **23,** 2831–2836
38. Bouadloun, F., Donner, D., and Kurland, C. G. (1983) Codon-specific missense errors *in vivo*. *EMBO J.* **2,** 1351–1356
39. Edelmann, P., and Gallant, J. (1977) Mistranslation in *E. coli*. *Cell* **10,** 131–137
40. Ross-Inta, C., Tsai, C. Y., and Giulivi, C. (2008) The mitochondrial pool of free amino acids reflects the composition of mitochondrial DNA-encoded proteins: indication of a post-translational quality control for protein synthesis. *Biosci. Rep.* **28,** 239–249
41. Dock-Bregeon, A. C., Rees, B., Torres-Larios, A., Bey, G., Caillet, J., and Moras, D. (2004) Achieving error-free translation; the mechanism of proofreading of threonyl-tRNA synthetase at atomic resolution. *Mol. Cell* **16,** 375–386
42. Holzwarth, G., and Doty, P. (1965) The ultraviolet circular dichroism of

polypeptides. *J. Am. Chem. Soc.* **87,** 218–228
43. Liu, Y., Satz, J. S., Vo, M. N., Nangle, L. A., Schimmel, P., and Ackerman, S. L. (2014) Deficiencies in tRNA synthetase editing activity cause cardioproteinopathy. *Proc. Natl. Acad. Sci. U.S.A.* **111,** 17570–17575
44. Hussain, T., Kruparani, S. P., Pal, B., Dock-Bregeon, A. C., Dwivedi, S., Shekar, M. R., Sureshbabu, K., and Sankaranarayanan, R. (2006) Post-transfer editing mechanism of a D-aminoacyl-tRNA deacylase-like domain in threonyl-tRNA synthetase from archaea. *EMBO J.* **25,** 4152–4162
45. Korencic, D., Ahel, I., Schelert, J., Sacher, M., Ruan, B., Stathopoulos, C., Blum, P., Ibba, M., and Söll, D. (2004) A freestanding proofreading domain is required for protein synthesis quality control in Archaea. *Proc. Natl. Acad. Sci. U.S.A.* **101,** 10260–10265
46. Guitart, T., Leon Bernardo, T., Sagalés, J., Stratmann, T., Bernués, J., and Ribas de Pouplana, L. (2010) New aminoacyl-tRNA synthetase-like protein in insecta with an essential mitochondrial function. *J. Biol. Chem.* **285,** 38157–38166
47. Claros, M. G., and Vincens, P. (1996) Computational method to predict mitochondrially imported proteins and their targeting sequences. *Eur. J. Biochem.* **241,** 779–786